

# Accepted Manuscript

The influence of photoperiod and light intensity on the growth and photosynthesis of *Dunaliella salina* (chlorophyta) CCAP 19/30

Yanan Xu, Iskander M. Ibrahim, Patricia J. Harvey



PII: S0981-9428(16)30191-7

DOI: [10.1016/j.plaphy.2016.05.021](https://doi.org/10.1016/j.plaphy.2016.05.021)

Reference: PLAPHY 4552

To appear in: *Plant Physiology and Biochemistry*

Received Date: 2 March 2016

Revised Date: 16 May 2016

Accepted Date: 16 May 2016

Please cite this article as: Y. Xu, I.M. Ibrahim, P.J. Harvey, The influence of photoperiod and light intensity on the growth and photosynthesis of *Dunaliella salina* (chlorophyta) CCAP 19/30, *Plant Physiology et Biochemistry* (2016), doi: 10.1016/j.plaphy.2016.05.021.

This is a PDF file of an unedited manuscript that has been accepted for publication. As a service to our customers we are providing this early version of the manuscript. The manuscript will undergo copyediting, typesetting, and review of the resulting proof before it is published in its final form. Please note that during the production process errors may be discovered which could affect the content, and all legal disclaimers that apply to the journal pertain.

1 The influence of photoperiod and light intensity on the growth and photosynthesis of *Dunaliella*  
2 *salina* (chlorophyta) CCAP 19/30  
3  
4 Yanan Xu, Iskander M. Ibrahim, and Patricia J. Harvey\*  
5  
6 University of Greenwich, Faculty of Engineering and Science, Central Avenue, Chatham Maritime,  
7 Kent, ME4 4TB, UK  
8  
9  
10 \*Author for Correspondence: Prof. Patricia J. Harvey, University of Greenwich, Faculty of  
11 Engineering and Science, Central Avenue, Chatham Maritime, Kent, ME4 4TB, UK  
12 Tel: +44-20-8331-9972  
13 E-mail: p.j.harvey@greenwich.ac.uk  
14

1 **Abstract**

2           The green microalga *Dunaliella salina* survives in a wide range of salinities via mechanisms  
3 involving glycerol synthesis and degradation and is exploited for large amounts of nutraceutical  
4 carotenoids produced under stressed conditions. In this study, *D. salina* CCAP 19/30 was cultured  
5 in varying photoperiods and light intensities to study the relationship of light with different growth  
6 measurement parameters, with cellular contents of glycerol, starch and carotenoids, and with  
7 photosynthesis and respiration. Results show CCAP 19/30 regulated cell volume when growing  
8 under light/dark cycles: cell volume increased in the light and decreased in the dark, and these  
9 changes corresponded to changes in cellular glycerol content. The decrease in cell volume in the  
10 dark was independent of cell division and biological clock and was regulated by the photoperiod of  
11 the light/dark cycle. When the light intensity was increased to above  $1000 \mu\text{mol photons} \cdot \text{m}^{-2} \cdot \text{s}^{-1}$ ,  
12 cells displayed evidence of photodamage. However, these cells also maintained the maximum level  
13 of photosynthesis efficiency and respiration possible, and the growth rate increased as light intensity  
14 increased. Significantly, the intracellular glycerol content also increased, >2-fold compared to the  
15 content in light intensity of  $500 \mu\text{mol photons} \cdot \text{m}^{-2} \cdot \text{s}^{-1}$ , but there was no commensurate increase in  
16 the pool size of carotenoids. These data suggest that in CCAP 19/30 glycerol stabilized the  
17 photosynthetic apparatus for maximum performance in high light intensities, a role normally  
18 attributed to carotenoids. ~~Taken together with the oscillatory changes in glycerol content with the~~  
19 ~~light/dark cycle it is proposed that glycerol plays a role not only in maintaining osmotic~~  
20 ~~homeostasis in CCAP 19/30, but also in maintaining metabolic homeostasis according to light~~  
21 ~~intensity.~~

22  
23 **Keywords:** *Dunaliella salina* CCAP 19/30, glycerol, light intensity, photoperiod, photosynthesis,  
24 stress

25

2 Microalgae are a source of a variety of natural products (Priyadarshani and Rath, 2012;  
3 Spolaore et al., 2006) including high value nutraceuticals, the exploitation of which started in the  
4 1970's, with the use of *Dunaliella salina* for the production of  $\beta$ -carotene, an antioxidant and a  
5 precursor of vitamin A (Raja et al., 2008). Carotenoids are essential for photosynthesis within algal  
6 chloroplasts: they are involved in both the light harvesting and photoprotecting processes, and in  
7 stabilizing the structure of photosynthetic pigment-protein complexes and aiding in their function  
8 (Mimuro and Akimoto, 2003; Mulders et al., 2014). The halotolerant *Dunaliella* genus comprises  
9 green microalgae that have been intensively studied for the production of  $\beta$ -carotene as a valuable  
10 compound for the health food industry (Ben-Amotz et al., 1982a; Davidi et al., 2014; Tafreshi and  
11 Shariati, 2009). *Dunaliella* algae differ from many green algal species as their cells lack a rigid  
12 polysaccharide cell wall and are bounded only by a cytoplasmic membrane, which allows them to  
13 adjust their volume and shape rapidly in response to hypo- or hyper-osmotic changes (Sadka et al.,  
14 1989; Zelazny et al., 1995). *Dunaliella* also produces glycerol in a salt medium via photosynthesis  
15 and the level of intracellular glycerol has been found to be proportional to the extracellular salt  
16 concentration, reaching above 50 % of the dry cell weight (Ben-Amotz et al., 1982b).

17 In the natural environment, all life is exposed to a daily cycle of light and dark fluctuation of  
18 light intensities and seasonal oscillation of daylight length as a result of the rotation of the planet.  
19 Eukaryotic and prokaryotic cells have evolved to respond to the rhythmic changes in environmental  
20 conditions and synchronize their cellular processes to the most appropriate time of the day (Dixon  
21 et al., 2014; Duanmu et al., 2014). Research on the green microalga *Chlamydomonas reinhardtii*  
22 shows that a wide range of biological processes including cell division, phototaxis, chemotaxis, cell  
23 adhesion, and nitrogen metabolism can be regulated by the natural clock and environmental  
24 conditions (Matsuo and Ishiura, 2011). Apart from the regulation of biological processes, both the  
25 yield and the composition of algal biomass are dependent on environmental light conditions. For  
26 example, starch synthesis and degradation in the marine microalga *Ostreococcus tauri* showed a

1 diurnal pattern with maximum starch content obtained towards the end of the day when cultured  
2 under a 12 h light/12 h dark cycle (Sorokina et al., 2011).

3 In industrial algal cultivations, illumination conditions such as continuous light or a light  
4 dark cycle, the length of the photoperiod and the light intensity affect both the growth of microalgae  
5 and the biomass composition (Wahidin et al., 2013). Continuous illumination in a photobioreactor  
6 system is often used to maximize the biomass production; however, excess light energy that cannot  
7 be converted into chemical energy induces photoinhibition damage to the algal photosynthetic  
8 apparatus, and inhibits the growth of algal cells (Baroli and Melis, 1998; Mulders et al., 2014). The  
9 provision of appropriate light and dark periods is therefore likely to be essential for both the growth  
10 of *D. salina* and optimum yields of target products. So far, despite the fact that intensive research  
11 has been carried out on the response of various *Dunaliella* strains to changes in environmental salt  
12 concentrations (Alkayal et al., 2010; Goyal, 2007a; 2007b; Lin et al., 2013; Zhao et al., 2013),  
13 limited information has been reported on the strain *D. salina* CCAP 19/30 in terms of its growth  
14 under varying light cycles and intensities.

15 To explore the effect of light period and light intensity on the regulation of growth,  
16 photosynthesis and biomass composition of CCAP 19/30, cells were cultured under a range of  
17 light/dark periods within a 24 h cycle and different light intensities and different markers of growth  
18 compared with those under continuous light. Photosynthesis of the cells was monitored in relation  
19 to light conditions along with the cellular content of photosynthesis-related biomass compounds  
20 including chlorophyll, carotenoids, protein, glycerol and starch. Understanding how regulation of  
21 light conditions and diurnal control helps to improve the production of algal biomass and desired  
22 bioproducts will guide treatment with suitable stressors and determine the time for treatment or  
23 harvesting of the algal biomass.

24

## 25 **2. Material and methods**

### 26 *2.1 Algal strain and cell cultures*

2 of Algae and Protozoa (CCAP, Scotland, UK). Our previous study has shown the strain CCAP  
3 19/30 grows best in medium with the salinity of 0.5 M NaCl and identical growth curves were  
4 obtained when carbon sources were provided by either 10 mM NaHCO<sub>3</sub> in the medium or  
5 continuous supply of 5 % CO<sub>2</sub>. Therefore in this study algae were cultured in Modified Johnsons  
6 Medium (J/1) (Borowitzka, 1988) containing 0.5 M NaCl and 10 mM NaHCO<sub>3</sub> with pH adjusted to  
7 7.5 by 10 mM Tris-buffer. Algae were maintained on 2 % agar plates in a temperature controlled  
8 growth chamber at (20 ± 2) °C. Illumination was provided under a 12 h light, 12 h dark cycle by  
9 cool white fluorescent lamps with a light intensity of ~50 μmol photons · m<sup>-2</sup> · s<sup>-1</sup>. Small stock  
10 cultures with ~25 ml medium were grown to mid-log phase by inoculation from algal colonies on  
11 agar plates. Stock cultures were then diluted 1 in 50 (v/v) as inoculum for larger cultures in each  
12 experiment. For algal cultivation, Erlenmeyer flasks containing 500 ml medium each were  
13 maintained at 25 °C with continuous shaking (100 rpm) in an ALGEM Environmental Modeling  
14 Labscale Photobioreactor (Algenuity, UK), which enables algae to grow under closely controlled  
15 conditions of light, temperature and mixing level. LEDs located at the bottom of the bioreactor  
16 chamber support the photosynthetic growth of algae by providing white, red or blue light at  
17 controlled light intensities.

18 To explore the effect of various photoperiods, a stock culture was set up under 12 h light/12  
19 h dark condition (LD) in the Algem at 25 °C with continuous shaking (100 rpm). This stock culture  
20 was maintained for three days, and at the end of the dark period, 10 ml of the culture was inoculated  
21 into 1 litre flask containing 490 ml of the medium. Six cultures were inoculated and grown under  
22 various cycles over a 24 h period: continuous light (LL), 4 h light and 20 h dark (4/20 LD), 8 h light  
23 and 16 h dark (8/16 LD), 12 h light and 12 h dark (12/12 LD), 16 h light and 8 h dark (16/8 LD) and  
24 20 h light and 4 h dark (20/4 LD). Under LL and 12/12 LD conditions, cell growth under a range of  
25 light intensities (50, 100, 200, 500, 1000 and 1500 μmol photons · m<sup>-2</sup> · s<sup>-1</sup>) was compared. Each  
26 growth condition was set up at least in triplicate. Cell growth was monitored automatically in the  
27 bioreactor by recording the value obtained for light scatter at 725 nm in OD units, with a time

1 interval of 1 h between measurements during the culture period. Cell concentration was determined  
2 by counting the cell number in culture broth using a haemocytometer.

3 Specific growth rate ( $\mu$ ) and doubling time ( $T_d$ ) of all cultures were calculated according to  
4 values of  $OD_{725nm}$  recorded using the data output of the photobioreactor in order to characterize the  
5 cell growth at various conditions. The specific growth rate ( $\mu$ ) of the algal growth and doubling  
6 time ( $T_d$ ) were calculated according to:

$$7 \mu = (\ln OD_t - \ln OD_0) / \Delta t,$$

$$8 T_d = \ln 2 / \mu,$$

9 where  $OD_t$  and  $OD_0$  refer to optical density at time t (h) and time zero respectively.

10

## 11 2.2 Cell volume analysis

12 Cell number and cell size distribution of cultures under LL or 12/12 LD conditions were  
13 measured with a BD Accuri™ C6 flow cytometer (BD biosciences, USA) as described by (Barker  
14 et al., 2012). Cell size can be quantitatively obtained by accurately measuring the forward-angle  
15 light scatter (FSC) signals of the algal culture broth and compare the mean FSC values obtained  
16 from samples and calibrating beads of known diameters. Images of cells grown under various light  
17 intensities were taken using a cell counter (Celeromics Technologies 1300) connected to a  
18 microscope and analyzed to calculate the average cell volume of each condition. At least 100 cells  
19 were taken in the image of each culture condition and the average cell volume of all measurements  
20 was taken. The cell volume was calculated based on the method described by Sun and Liu (Sun and  
21 Liu, 2003). By assuming *Dunaliella* cells have a geometric shape of prolate spheroid, the  
22 biovolumes of CCAP 19/30 cells cultured under various light intensities were calculated according  
23 to the equation:

$$24 V = \pi/6 * d^2 * h,$$

25 where d is the diameter of cross section and h is the diameter of apical section of a subspherical  
26 body.

27

2 Cells were harvested at 3 h intervals over a 24 h period to determine the cellular content of  
3 the target products: glycerol, chlorophyll and carotenoids. Based on our previous study, cells  
4 harvested by centrifugation at 3000 G would not be damaged and glycerol remained in cell pellets  
5 (Xu et al., 2015), therefore, 1 ml of culture samples were taken and centrifuged at 3000 G for 5 min  
6 to get the cell pellets. The pellets were then resuspended in 1 ml of distilled water and 200  $\mu$ l of  
7 chloroform and vigorously vortexed to extract the glycerol. The water phase containing glycerol  
8 was separated from chloroform by centrifugation at 10,000 G for 10 min and the glycerol  
9 concentration in the water phase was determined according to the following procedure (Bondioli  
10 and Bella, 2005): A series of glycerol standards with various concentrations were prepared first to  
11 generate standard curves. Each working standard and the samples were treated with 1.2 ml of a 10  
12 mM sodium periodate solution and shaken for 30 seconds. Each solution was then treated with 1.2  
13 ml of a 0.2 M acetylacetone solution, placed in a water bath at 70 °C for 1 minute and stirred  
14 manually. The solutions were immediately placed in cold water to stop the reaction and the  
15 absorbance was measured using a UV/Vis spectrometer at wavelength of 410 nm.

16 Cellular protein content was determined using the Total protein kit, Micro Lowry,  
17 Peterson's Modification (Sigma-Aldrich Co. LLC.) according to manufacturer's instructions.  
18 Cellular starch content was measured using Total Starch Assay Kit (Megazyme, Ireland) according  
19 to the manufacturer's instructions.

20 Pigments were extracted from harvested biomass using 80 % (v/v) acetone. The absorbance  
21 of acetone extract without cell debris was measured at wavelength of 480 nm for total carotenoids.  
22 The content of total carotenoids was calculated according to Strickland & Parsons (Strickland and  
23 Parsons, 1972):

$$24 \text{ Total Carotenoids } (\mu\text{g} \cdot \text{ml}^{-1}) = 4.0 * \text{Abs}_{480\text{nm}},$$

25 where  $\text{Abs}_{480\text{nm}}$  is the absorbance of 80 % acetone extract measured at 480 nm.

26 Chlorophyll a, b and total Chlorophyll were evaluated by measuring the absorbance of the  
27 acetone extract at 664 nm and 647nm and calculated according to Porra et al. (Porra et al., 1989):

1 Chl a ( $\mu\text{g} \cdot \text{ml}^{-1}$ ) =  $(12.25 * \text{Abs}_{664\text{nm}}) - (2.55 * \text{Abs}_{647\text{nm}})$ ;

2 Chl b ( $\mu\text{g} \cdot \text{ml}^{-1}$ ) =  $(20.31 * \text{Abs}_{647\text{nm}}) - (4.91 * \text{Abs}_{664\text{nm}})$ ,

3 Total Chl ( $\mu\text{g} \cdot \text{ml}^{-1}$ ) = Chl a ( $\mu\text{g} \cdot \text{ml}^{-1}$ ) + Chl b ( $\mu\text{g} \cdot \text{ml}^{-1}$ ),

4 where  $\text{Abs}_{647\text{nm}}$  and  $\text{Abs}_{664\text{nm}}$  refer to the absorbance of the 80 % acetone extract measured at 664  
5 nm and 647 nm respectively.

6 A sine wave equation trend-line was fitted to the data for cell size, cell glycerol content and  
7 cell starch content using Microsoft Excel 2013 solver to optimise A, f and k by minimising the sum  
8 of the square of the differences between the results derived from the experimental data and those  
9 calculated from the equations, for the sine wave described by equation:

$$y = A \sin(2\pi ft + k) + B$$

10 Where A is the amplitude, f is frequency (day<sup>-1</sup>), t is time (day), k is a phase shift constant and B  
11 is the overall average value.

12

#### 13 2.4 Oxygen evolution and dark respiration

14 Cells were harvested during the exponential growth phase and  $\text{NaHCO}_3$  was added to a final  
15 concentration of 10 mM 5 minutes before the start of each measurement. The rate of net  $\text{O}_2$   
16 evolution and dark respiration were measured as described by Brindley et al. (Brindley et al., 2010)  
17 at 25 °C by a Clark-type electrode (Hansatech)(Delieu and Walker, 1983).  $\text{O}_2$  evolution was  
18 induced with  $1500 \mu\text{mol photons} \cdot \text{m}^{-2} \cdot \text{s}^{-1}$  actinic light. After an initial period of 30 minutes of  
19 dark adaption,  $\text{O}_2$  evolution was measured for 5 minutes followed by dark respiration for 20  
20 minutes. The average net rate of photosynthesis was then determined from the oxygen gradient over  
21 5 minute,  $d\text{O}_2/dt$ . Dark respiration was determined by following the same procedure, except that it  
22 was calculated using the data from the last 5 minutes of the 20 min experiment. Sodium dithionite  
23 was used to calibrate the electrode.

24

#### 25 2.5 Room temperature fluorescence

1 The maximum quantum yield of photosystem II was measured using a Walz PAM 101  
2 fluorometer with the 101-ED emitter-detector unit. Walz Optical Unit ED-101US was used for cell  
3 suspension. All samples were grown to an  $OD_{725nm}$  of  $\sim 0.5$ . Actinic light for state-2 to state-1  
4 transitions was provided by Flexilux 150 HL white light behind a blue Corning 4-96 glass filter.  
5 Prior to measurement cells were dark-adapted for 5 minutes. Minimum fluorescence ( $F_0$ ) was  
6 determined by illuminating with measuring light ( $0.01 \mu\text{mol photons} \cdot \text{m}^{-2} \cdot \text{s}^{-1}$ ). Maximum  
7 fluorescence ( $F_m$ ) for dark-adapted state was determined with 0.8 second long saturation ( $6500$   
8  $\mu\text{mol photons} \cdot \text{m}^{-2} \cdot \text{s}^{-1}$ ) pulse delivered from a Schott KL 1500 white light source. The actinic light  
9 was then turned on and a second saturation pulse was applied after 20 minutes ( $F'_m$ ). At the end of  
10 state transitions measurement, actinic light was turn off to obtain  $F'_0$ . The maximum quantum yield  
11 of PSII ( $F_v/F_m$ ) was calculated as  $(F_m - F_0)/F_m$ ; The effective quantum yield of PSII ( $\Phi_{PSII}$ ) was  
12 calculated as  $(F'_m - F_t)/F'_m$ ; Photochemical quenching (qP) was calculated as  $(F'_m - F_t)/(F'_m - F'_0)$   
13 (Genty et al., 1989).

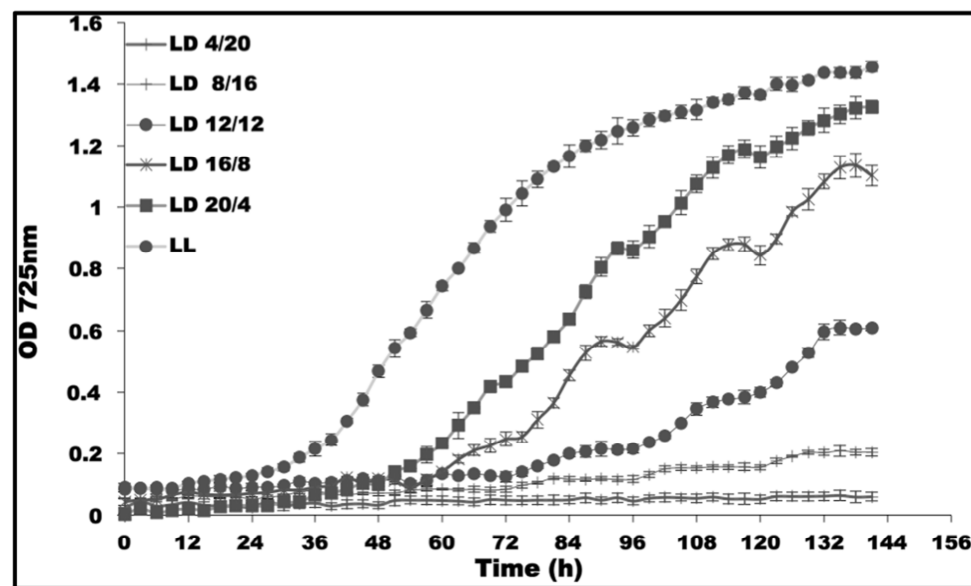
14

### 15 3. Results

#### 16 3.1 Growth of CCAP 19/30 under continuous light and light/dark cycles with various photoperiods

17 To investigate the effect of different photoperiod on the growth of CCAP 19/30, cultures  
18 were exposed to 24 h light/dark (LD) cycles with different photoperiods and also continuous light  
19 (LL). Results are shown in Fig. 1 (see also Supplementary Material Table I). The light periods were  
20 4, 8, 12, 16, 20 and 24 hours in every 24 hours (4/20 LD, 8/16 LD, 12/12 LD, 16/8 LD, 20/4 LD  
21 and LL respectively) with the light intensity of  $200 \mu\text{mol photons} \cdot \text{m}^{-2} \cdot \text{s}^{-1}$ . The data show that  
22 cultures grown under different light conditions showed different overall growth rates over the six  
23 days monitored. The longer the photoperiod that the cultures were exposed to, the faster the growth  
24 rates and the higher the cell densities that could be obtained. Moreover, different growth rates were  
25 obtained in the light periods and the dark periods for cultures grown in LD cycles. Algae grown in  
26 all LD cycle conditions presented a clear rhythmic oscillation in the optical density of the culture  
27 broth (Fig. 1). Light scatter at 725 nm was used as a measure of the biomass concentration of the

1 cultures and increased in all light periods but decreased in all dark periods. This oscillation in the  
2 optical density was absent in cultures grown under continuous light. Besides, this oscillation was  
3 found to respond exactly to the rhythmic changes of the light conditions in all LD cultures despite  
4 the length of the photoperiods (Fig. 1).  
5



6  
7 **Fig. 1.** Growth of CCAP 19/30 exposed to various 24 h cycles with different photoperiods (4/20 LD,  
8 8/16 LD, 12/12 LD, 16/8 LD, 20/4 LD and LL). All cultures were grown at 25 °C with continuous  
9 shaking (100 rpm). The light intensity during the light periods of all conditions was 200  $\mu\text{mol}$   
10  $\text{photons} \cdot \text{m}^{-2} \cdot \text{s}^{-1}$ . Cultures in each condition were set up at least in triplicate and shown in figure  
11 are means of the measurement  $\pm$  standard deviation.

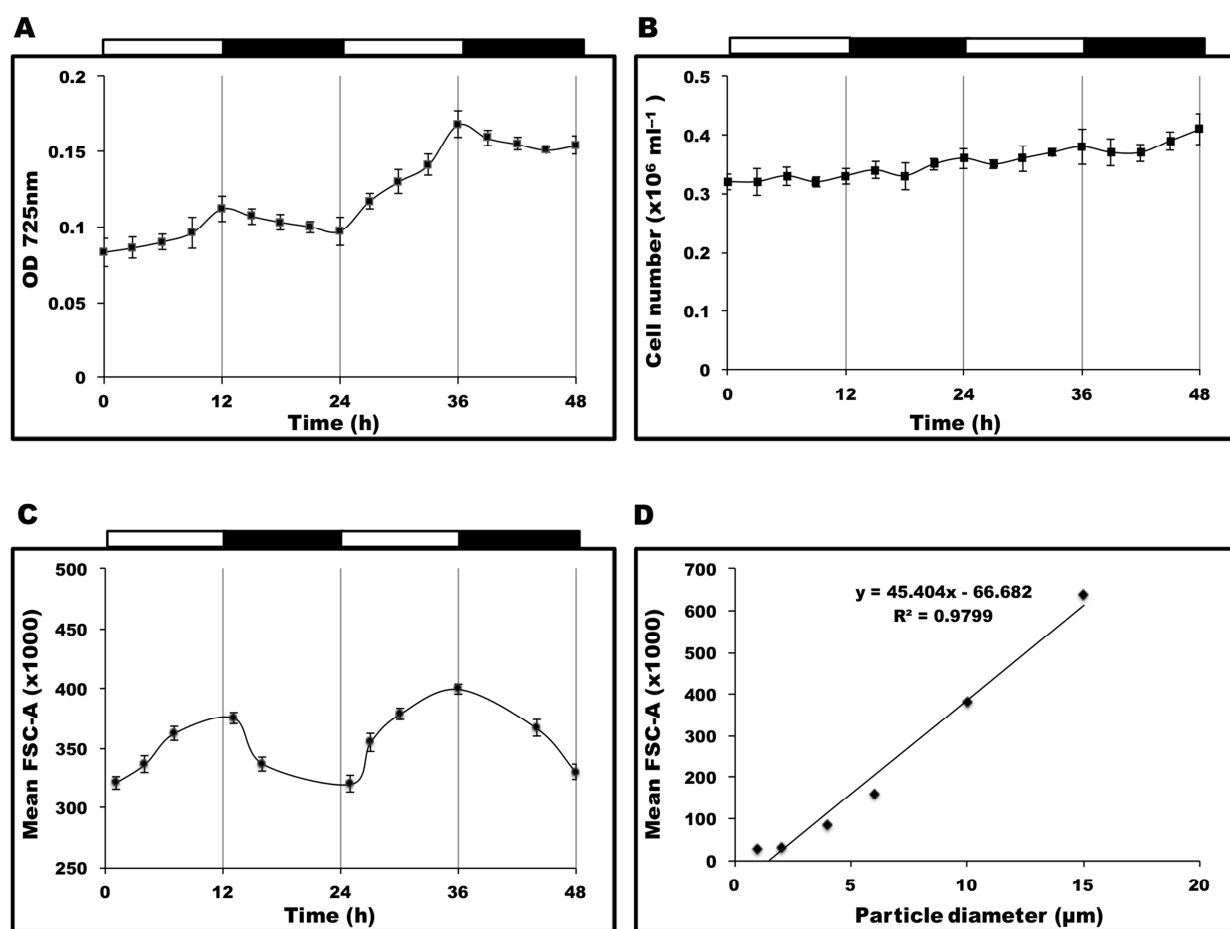
### 13 3.2 Cell volume of CCAP 19/30 is controlled by light/dark cycles

14 The cell density, optical density and cell volume of CCAP 19/30 cultures were monitored  
15 over a 48 h period when cultured under 12/12 LD conditions with the light intensity of 200  $\mu\text{mol}$   
16  $\text{photons} \cdot \text{m}^{-2} \cdot \text{s}^{-1}$  during the light periods. As shown in Fig. 2A, over the 48 h period monitored, the  
17 optical density of the respective cultures showed clear oscillations and increased in the light periods  
18 and decreased in the dark periods. However, in Fig. 2B cell number of the cultures slightly

1 increased both in the light and dark periods. If the total biovolume is evaluated by multiplying the  
2 average cell volume with the cell number, it can be concluded that the average cell volume must  
3 also decrease in the dark period in order for the optical density to decrease while the cell number  
4 increases. As a result, the decrease in optical density suggests either the division of mother cells into  
5 smaller daughter cells or an actual reduction in the cell volume. Cell division could explain why the  
6 optical density remained relatively unchanged during the dark in the first few days when the cell  
7 density was low. However, after cell density increased, the optical density had a significant  
8 decrease during the dark period despite the length of the photoperiods (Fig. 1), indicating cell  
9 division was not the main reason that cells in the dark had smaller cell volumes. The more likely  
10 explanation was that algal metabolism during the LD cycle caused oscillations in the cellular  
11 content of osmolytes such as glycerol, which further induced the oscillation in the cell volume over  
12 the cycle. Cultures under continuous light were changed to LD conditions at the end of the log  
13 phase and the optical densities started to show the oscillation once the cultures were placed in the  
14 dark (data not shown), confirming that the decrease in optical density was only caused by absence  
15 of light.

16 Flow cytometry was used to monitor cell numbers and measure the cell diameter of CCAP  
17 19/30 cells grown under 12/12 LD cycles in order to find out whether the oscillation of biomass  
18 density (optical density of the culture broth) was caused by changes in cell volumes. By running a  
19 series of calibrating beads sizing from 1 to 15  $\mu\text{m}$  in diameter, it can be seen that the mean forward-  
20 angle light scatter (FSC-A) signal is in a high linear relationship with the particle size (Fig. 2D).  
21 Thus the FSC-A values of cultures grown over the 48 h LD cycles as shown in Fig. 2C prove that  
22 the cell diameter increased during the light periods and decreased in the dark periods.

23



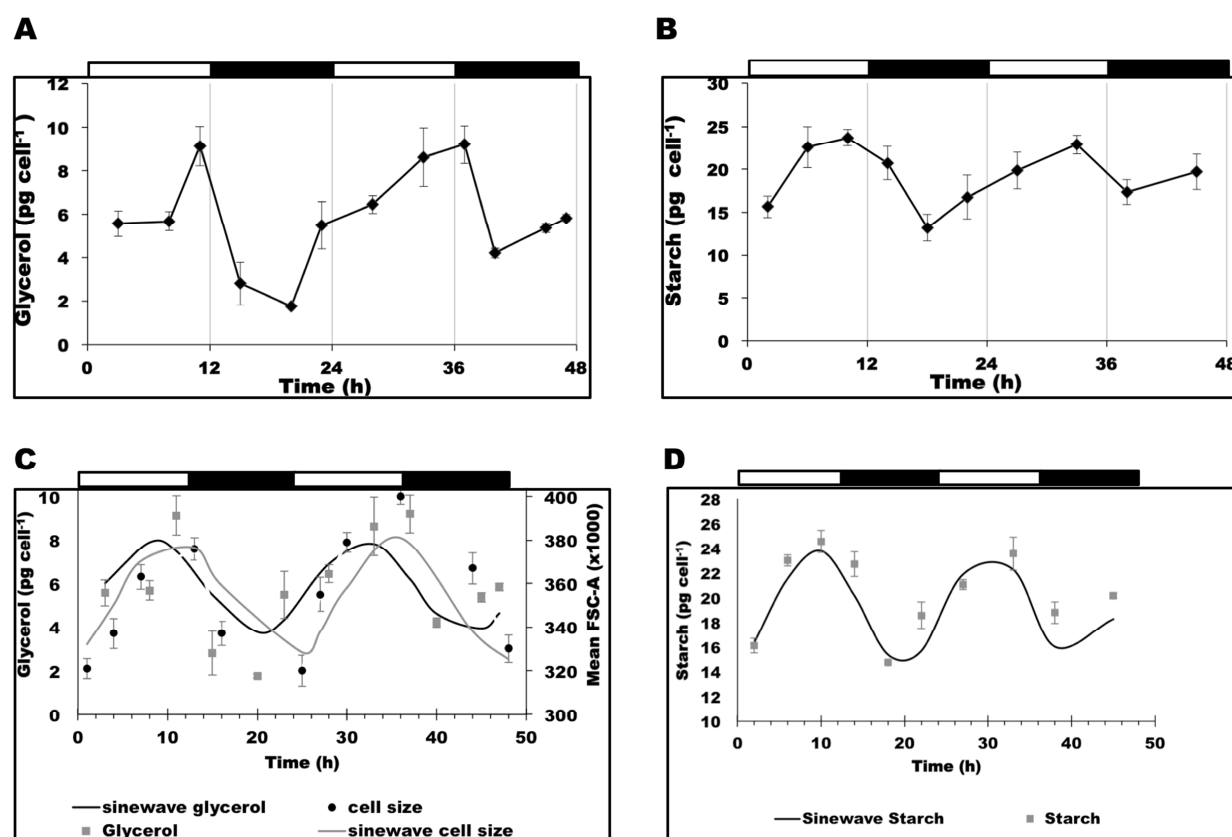
1  
 2 **Fig. 2.** (A) Changes in the optical density of CCAP 19/30 cultures within 48 h period when growing  
 3 under 12/12 LD conditions. (B) Changes in the cell density of CCAP 19/30 cultures within 48 h  
 4 period when growing under 12/12 LD conditions. (C) Changes in the mean forward-angle light  
 5 scatter (FSC-A) signals of CCAP 19/30 cells within 48 h period when growing under 12/12 LD  
 6 conditions monitored by flow cytometer. (D) Standard curve of mean FSC-A signal to particle size  
 7 showing that mean FSC-A signal is highly correlated with particle size. All cultures were grown at  
 8 25 °C with continuous shaking (100 rpm). The light intensity during the light periods of all  
 9 conditions was  $200 \mu\text{mol photons} \cdot \text{m}^{-2} \cdot \text{s}^{-1}$ . Cultures in each condition were set up at least in  
 10 triplicate.

11  
 12 **3.3 Cellular glycerol and starch content increased in light and decreased in dark**

13 Glycerol is one of the most important osmolytes in *Dunaliella* cells that regulate the changes  
 14 in cell volume. *Dunaliella* species are able to accumulate a significant amount of intracellular

1 glycerol in response to the extracellular osmotic pressure (Ben-Amotz and Avron, 1981; Chitlaru  
2 and Pick, 1991). In the present study, extracellular osmotic conditions were held constant, and  
3 consequently the changes of cell volume during the LD cycles should reflect a similar oscillation in  
4 the cellular glycerol content so as to maintain constant intracellular osmotic conditions. As shown  
5 in Fig. 3A, cellular glycerol content of CCAP 19/30 grown under 12/12 LD cycles showed an  
6 oscillation changing within the range of 1.7 to 9.3 pg cell<sup>-1</sup>. The cellular glycerol content increased  
7 overall in the light periods tending to reach the maximum level around the end of the light periods.  
8 In the dark, glycerol content per cell decreased, then increased a few hours before the light period.  
9 It has been reported that the carbon source for glycerol synthesis in *Dunaliella* upon salt stress is  
10 contributed by both photosynthesis and starch degradation (Goyal, 2007b), so cellular starch content  
11 of CCAP 19/30 grown under 12/12 LD cycles was measured as shown in Fig. 3B. Cellular starch  
12 content over the LD cycles shows a similar pattern to cellular glycerol content in CCAP 19/30,  
13 namely, it increased in the light, then decreased in the dark and then increased some hours before  
14 return of the light period. The decrease then increase in the dark period in starch and glycerol  
15 contents per cell is noteworthy. As shown in Fig 3 (C) and (D), each of cell size, and cellular  
16 glycerol and starch contents varied over time in a sinusoidal manner, with the effects of time on  
17 each dependant variable being statistically significant ( $P < 0.001$ ). When the data were fitted to a  
18 sine wave function the time periods of the wave for each data set were calculated as 24.9 hours and  
19 23.3 hours for cell size and cellular glycerol content respectively, but only 20.7 hours for cellular  
20 starch content. Clearly many effects including additional dark-related events such as membrane  
21 lipid breakdown releasing glycerol may be involved in modulating starch and glycerol pool sizes in  
22 the dark. Nevertheless, overall the data suggest that the diurnal cycle of photosynthesis and  
23 respiration under 12/12 LD conditions would appear to play a major role in regulating the cycle of  
24 cellular glycerol and starch content.

25



1

2 **Fig. 3.** Changes of (A) cellular glycerol content and (B) total starch content of CCAP 19/30 cells  
 3 grown under 12/12 LD over a 48 h period. (C) and (D): Sine wave equation trend-line was fitted to  
 4 the data for cell size and cellular glycerol content (C), and cellular starch content (D). Cultures were  
 5 grown at 25 °C with continuous shaking (100 rpm) and the light intensity during the light periods  
 6 was  $200 \mu\text{mol photons} \cdot \text{m}^{-2} \cdot \text{s}^{-1}$ . All cultures were set up at least in triplicate and shown in figure  
 7 are means of the measurement  $\pm$  standard deviation.

8

9 *3.4 Growth of CCAP 19/30 under light/dark cycles with different light intensities*

10 Comparing the growth of CCAP 19/30 under continuous light and various LD cycles in Fig.  
 11 1, it is apparent that under continuous light, algal growth rate is significantly improved since the  
 12 carbon assimilation rate is higher with more light energy received by the cells. Increasing the light  
 13 intensity should therefore increase the algal growth rate. As shown in Fig. 4, when increasing the  
 14 light intensity from  $50$  to  $1500 \mu\text{mol photons} \cdot \text{m}^{-2} \cdot \text{s}^{-1}$ , the growth rate of CCAP 19/30 increased  
 15 rapidly with the increase in light intensity in both LD and LL light conditions. Fig. 4 also shows that

1 during the dark periods (12-24 h and 36-48 h), the optical densities of cultures grown under the LD  
 2 cycles decreased markedly in contrast to the situation for cultures grown under continuous light,  
 3 which is consistent with the result shown in Fig. 1.

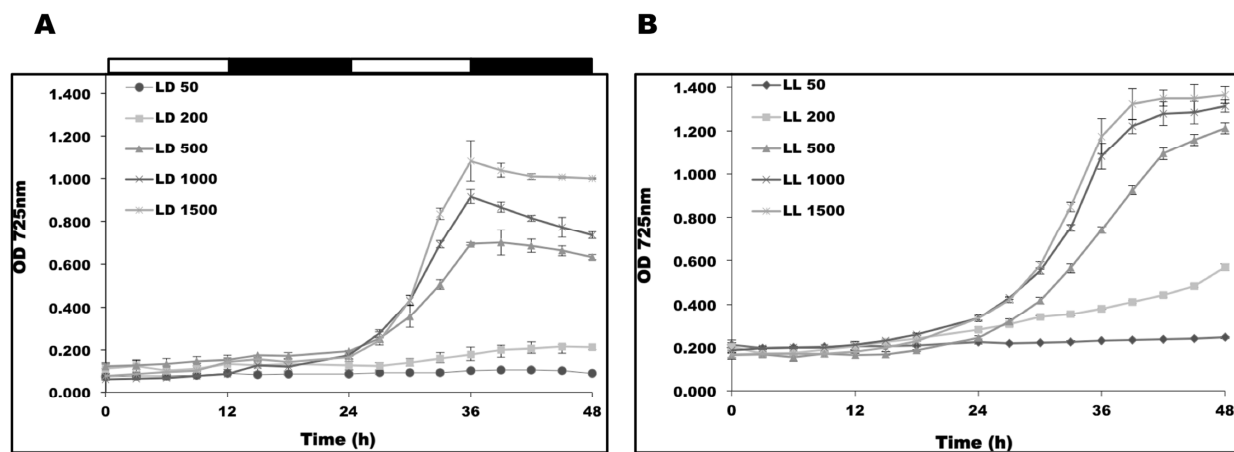
4 Table 1 compares the doubling times, obtained by calculating the maximum specific growth  
 5 rate, for CCAP cultures grown either under a period of either continuous light at different light  
 6 intensities or under the LD cycle. Since the growth rate in the light period differs from that in the  
 7 dark phase only the light period growth rates were used. These data together with those in Fig. 4  
 8 show that although under continuous light, cultures could reach high cell densities in a shorter time,  
 9 which means a faster overall growth rate, cultures grown under LD cycles actually grew slightly  
 10 faster in the light period than cultures under continuous light, indicating that cells grown in a LD  
 11 cycle condition are fine-tuned to carry out photosynthesis more efficiently than under continuous  
 12 light.

13

14 Table 1. Doubling times for cultures grown in either a continuous or a light/dark cycle with  
 15 different light intensities from 50 to 1500  $\mu\text{mol photons} \cdot \text{m}^{-2} \cdot \text{s}^{-1}$ . All samples were taken at mid  
 16 log phase of the cultures and at the end of the light periods. Data are means of at least three  
 17 experiments  $\pm$  standard deviation.

Light intensity ( $\mu\text{mol photons} \cdot \text{m}^{-2} \cdot \text{s}^{-1}$ )	Doubling time	
	Continuous light	Light/dark period
50	198.0 ( $\pm$ 19.1)	63.0 ( $\pm$ 11.2)
200	28.0 ( $\pm$ 2.8)	23.3 ( $\pm$ 2.1)
500	7.5 ( $\pm$ 0.1)	6.4 ( $\pm$ 0.2)
1000	7.2 ( $\pm$ 0.2)	5.0 ( $\pm$ 0.2)
1500	6.5 ( $\pm$ 0.3)	4.2 ( $\pm$ 0.1)

18



2

3 **Fig. 4.** Growth of CCAP 19/30 under (A) 12/12 LD and (B) LL conditions with various light  
 4 intensities during the light periods of 50, 200, 500, 1000 and 1500  $\mu\text{mol photons} \cdot \text{m}^{-2} \cdot \text{s}^{-1}$ . Cultures  
 5 were maintained at 25 °C with continuous shaking (100 rpm). Cultures in each condition were set  
 6 up at least in triplicate shown in figure are means of the measurement  $\pm$  standard deviation.

7

### 8 3.5 Major biomass compositions of CCAP 19/30 grown under various light intensities

9 *Dunaliella* species have been found to be carotenoid-accumulating strains such that the  
 10 carotenoids/chlorophyll ratio significantly increases upon high light stress. In the present study, the  
 11 pigment composition (total chlorophyll and carotenoids) of CCAP 19/30 grown under 12/12 LD  
 12 cycle with light intensities from 50 to 1500  $\mu\text{mol photons} \cdot \text{m}^{-2} \cdot \text{s}^{-1}$  was determined. As can be seen  
 13 in Table 1, with increasing light intensities, the cells appeared to be increasingly stressed based on  
 14 the reduction in content of both chlorophyll and carotenoids. Furthermore, the  
 15 carotenoids/chlorophyll ratio of CCAP 19/30 only slightly increased from low light to high light  
 16 (Table 2). By contrast, cellular glycerol content increased. Shown in Table 2, the glycerol content  
 17 of CCAP 19/30 cultures growing in LD conditions under various light intensities was monitored  
 18 during the mid-log phase of growth and at the end of the light period during a 24 h period when  
 19 glycerol reaches the maximum level. At low light when the light intensities were 50, 200 or 500  
 20  $\mu\text{mol photons} \cdot \text{m}^{-2} \cdot \text{s}^{-1}$ , the cellular glycerol content was maintained at similar levels (, however  
 21 when the light intensity increased to high light (1000 and 1500  $\mu\text{mol photons} \cdot \text{m}^{-2} \cdot \text{s}^{-1}$ ), the cellular

1 glycerol content increased >2-fold compared to the values at low light (Table 2). Unlike cellular  
 2 glycerol content, total starch and protein content of CCAP 19/30 cells grown under various light  
 3 intensities remained constant when increasing the light from 50 to 1500  $\mu\text{mol photons} \cdot \text{m}^{-2} \cdot \text{s}^{-1}$  as  
 4 shown in Table 2.

5

6 **Table 2.** Cellular content of chlorophyll, carotenoids, glycerol, starch and protein and average cell  
 7 volume of CCAP 19/30 cultures grown under 12/12 LD with different light intensities from 50 to  
 8 1500  $\mu\text{mol photons} \cdot \text{m}^{-2} \cdot \text{s}^{-1}$  during the light periods. All samples were taken at mid log phase of  
 9 the cultures and at the end of the light periods. Data are means of at least three experiments  $\pm$   
 10 standard deviation.

Light intensity ( $\mu\text{mol photons} \cdot \text{m}^{-2} \cdot \text{s}^{-1}$ )	Carotenoid s (pg cell <sup>-1</sup> )	Chlorophyll (pg cell <sup>-1</sup> )	Carotenoids / Chlorophyll	Glycerol (pg cell <sup>-1</sup> )	Starch (pg cell <sup>-1</sup> )	Protein (pg cell <sup>-1</sup> )	Average cell volume ( $\mu\text{m}^3$ )
50	0.81 $\pm$ 0.11	3.23 $\pm$ 0.45	0.25 $\pm$ 0.00	8.97 $\pm$ 1.66	20.16 $\pm$ 0.67	22.51 $\pm$ 2.24	175.60 $\pm$ 46.44
200	0.78 $\pm$ 0.13	3.65 $\pm$ 0.61	0.21 $\pm$ 0.00	12.06 $\pm$ 3.17	23.71 $\pm$ 0.85	22.44 $\pm$ 1.41	190.03 $\pm$ 56.48
500	0.58 $\pm$ 0.01	2.25 $\pm$ 0.11	0.26 $\pm$ 0.01	7.51 $\pm$ 1.05	20.64 $\pm$ 3.67	22.21 $\pm$ 2.03	179.32 $\pm$ 48.33
1000	0.56 $\pm$ 0.02	1.83 $\pm$ 0.10	0.31 $\pm$ 0.01	23.26 $\pm$ 3.94	21.86 $\pm$ 2.55	26.63 $\pm$ 4.08	202.19 $\pm$ 41.29
1500	0.53 $\pm$ 0.02	1.54 $\pm$ 0.07	0.34 $\pm$ 0.01	21.14 $\pm$ 4.02	20.72 $\pm$ 1.06	19.28 $\pm$ 2.39	210.72 $\pm$ 55.39

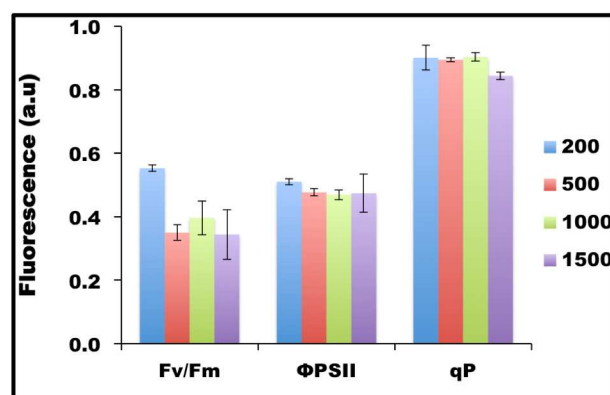
11

### 12 *3.6 Photosynthetic activities of CCAP 19/30 acclimated to various light intensities*

13 Prolonged exposure to high light is known to induce photodamage, resulting in less functional  
 14 photosystems and decrease in the photosynthetic yield (Baroli and Melis, 1998; Melis, 1999), yet  
 15 using OD<sub>725nm</sub> measurement, CCAP 19/30 appeared to grow optimally at high light intensities of  
 16 1000 and 1500  $\mu\text{mol photons} \cdot \text{m}^{-2} \cdot \text{s}^{-1}$ : these levels of light are normally considered to be  
 17 photodamaging for higher plants and other photosynthetic microorganisms (Havaux et al., 2000). In  
 18 order to gain more insight into the photosynthetic health of cells that had been fully acclimated to

1 light intensity ranging from 50 to 1500  $\mu\text{mol photons} \cdot \text{m}^{-2} \cdot \text{s}^{-1}$ , the quantum yield of photosystem  
 2 II (PSII), photochemical quenching, and oxygen evolution were investigated.

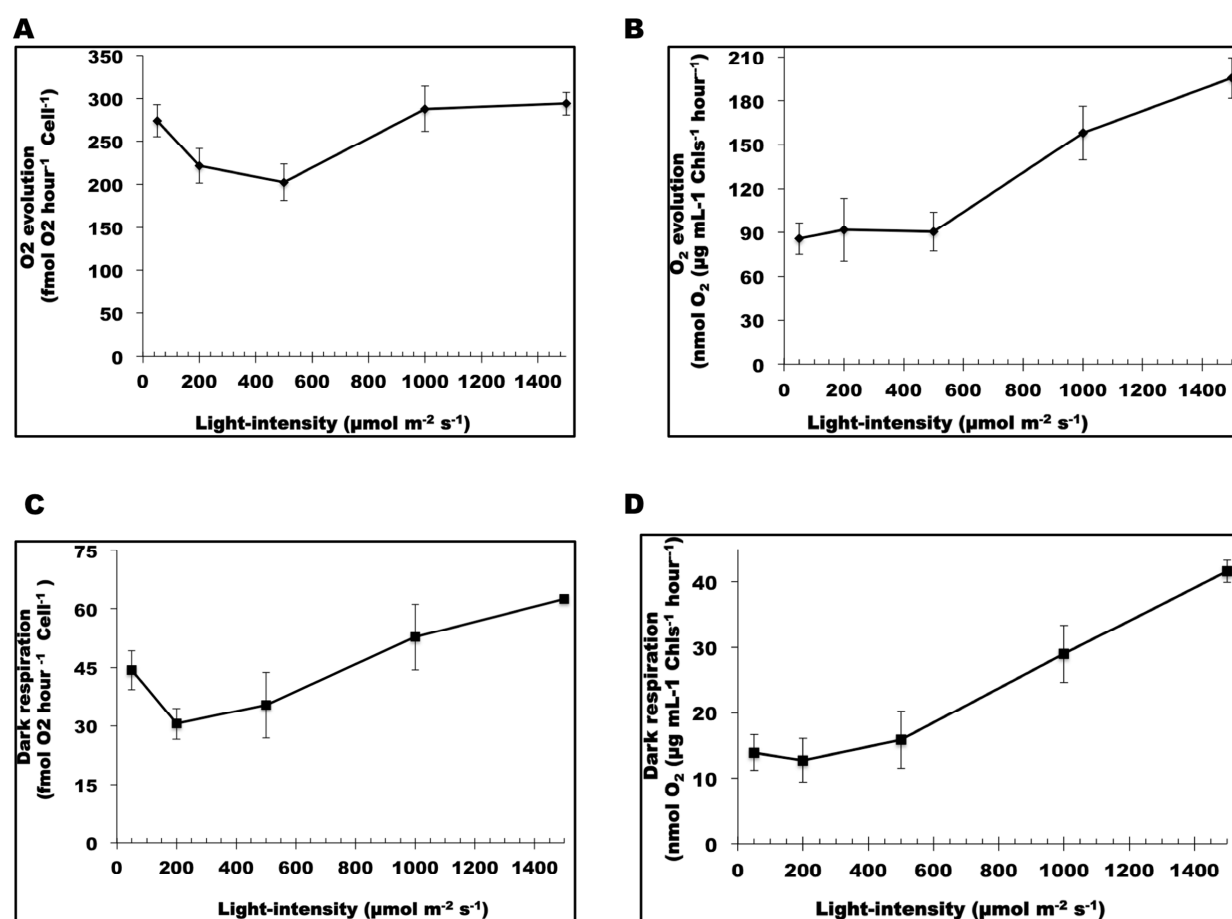
3 The quantum yield of PSII is measured by the ratio of  $F_v/F_m$ , and represents the maximum  
 4 potential quantum efficiency of PSII if all capable reaction centres were open. Fig. 5 shows that the  
 5  $F_v/F_m$  value decreased with increase in light intensity from  $\sim 0.55$  at 50 and 200  $\mu\text{mol photons} \cdot \text{m}^{-2}$   
 6  $\cdot \text{s}^{-1}$ , and reached a constant low value of between 0.3-0.4 for light intensities above 500  $\mu\text{mol}$   
 7  $\text{photons} \cdot \text{m}^{-2} \cdot \text{s}^{-1}$  (Fig. 5). In parallel,  $\text{O}_2$  evolution rate decreased from 50 to 500  $\mu\text{mol photons} \cdot$   
 8  $\text{m}^{-2} \cdot \text{s}^{-1}$  when normalized to cell number (Fig. 6A) or was unchanged when normalized to total  
 9 chlorophyll (Fig. 6B); remarkably, however,  $\text{O}_2$  evolution rate increased to a maximum level for  
 10 those cells acclimated to 1000 and 1500  $\mu\text{mol photons} \cdot \text{m}^{-2} \cdot \text{s}^{-1}$  (Fig. 6A and 6B).



11

12 **Fig. 5.** Pulse-modulated chlorophyll fluorescence measurements of quantum yield of PSII vs light  
 13 intensities. Photochemical quantum yield  $F_v/F_m$  for dark-adapted state was determined with cultures  
 14 acclimated to different light intensity.  $F_v/F_m$  was calculated as  $(F_m - F_0)/F_m$ . The effective quantum  
 15 yield of PSII ( $\Phi_{\text{PSII}}$ ) and photochemical quenching (qP) were calculated as  $(F'_m - F_t)/F'_m$  and  $(F'_m -$   
 16  $F_t)/(F'_m - F'_0)$ , respectively.

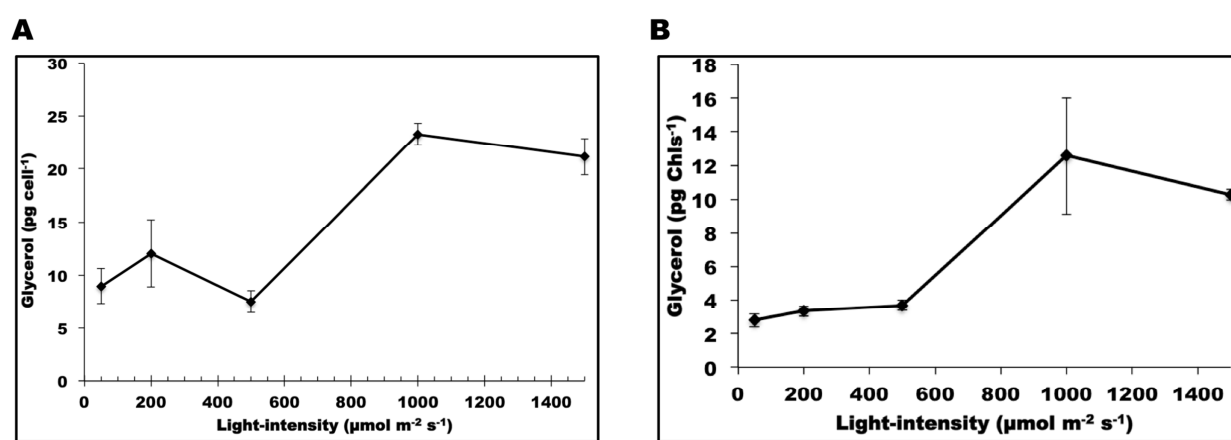
17



1  
2 **Fig. 6.** Oxygen evolution and dark respiration rates. Oxygen evolution (A and B) and dark  
3 respiration (C and D) rates with cells acclimated to different light intensities measured as in method  
4 and material section. A and C are normalized to cell number and B and D are normalized to  
5 chlorophyll. Each data point is the mean of three measurements  $\pm$  standard deviation.

6  
7 Photosynthetic efficiency is often calculated from fluorescence measurement as the product  
8 of effective quantum yield of open PSII center ( $\Phi_{\text{PSII}}$ ) and fraction of PSII centres in the open state  
9 (qP). Despite the decrease in the  $F_v/F_m$  with light intensity, other photosynthetic parameters such as  
10 effective  $\Phi_{\text{PSII}}$  and qP were relatively unchanged with increase in the light intensity (Fig. 5). Shown  
11 in Fig. 6C and 6D, dark respiration rate first decreased from 50 to 200  $\mu\text{mol photons} \cdot \text{m}^{-2} \cdot \text{s}^{-1}$ , then  
12 increased from 200 to 1500  $\mu\text{mol photons} \cdot \text{m}^{-2} \cdot \text{s}^{-1}$  (Fig. 6C and 6D). Shown in Fig. 7, the decrease  
13 in both photosynthesis and respiration from 50 to 200  $\mu\text{mol photons} \cdot \text{m}^{-2} \cdot \text{s}^{-1}$  was accompanied by  
14 glycerol synthesis and the cellular glycerol content increased. From 200 to 500  $\mu\text{mol photons} \cdot \text{m}^{-2} \cdot$

1  $s^{-1}$ , the increase in respiration rate with the decrease in photosynthesis coupled with the now  
2 declining cellular glycerol content suggested that cells started to use glycerol for respiration at 500  
3  $\mu\text{mol photons} \cdot \text{m}^{-2} \cdot \text{s}^{-1}$ . From 500 to 1000  $\mu\text{mol photons} \cdot \text{m}^{-2} \cdot \text{s}^{-1}$ , both photosynthesis and  
4 respiration increased remarkably, paralleling the increase in cellular glycerol concentration; while  
5 from 1000 to 1500  $\mu\text{mol photons} \cdot \text{m}^{-2} \cdot \text{s}^{-1}$ , photosynthesis became saturated and respiration  
6 continued to increase, most likely at the expense of glycerol, which declined in concentration.  
7 Taken together with the growth data, these data suggest that CCAP 19/30 cells adjust their  
8 photosystems to achieve maximum photosynthesis even when they are exposed to high light  
9 intensity and suffering photodamage. The link between photosynthetic efficiency and glycerol  
10 synthesis is shown clearly in Fig. 7, and suggests that glycerol plays an important role along with  
11 carotenoids (Table 1) in protecting cells from oxidative damage.



12  
13 **Fig. 7.** Glycerol content was determined as in the method and material section. A is normalized to  
14 cell number and B is normalized to total chlorophyll. Samples were taken at the end of the light  
15 periods for all measurement. Each data point is the mean of three measurements  $\pm$  standard  
16 deviation.

#### 18 **4. Discussion**

19 The work presented here shows that *D. salina* CCAP 19/30 cells alter their cell diameter in  
20 response to a light/dark cycle of light, and that the periodicity of change in cell diameter  
21 corresponds to change in cellular glycerol content. Results in Fig. 2 illustrate that the cells increase

1 in volume in the light periods and decrease in volume in the dark periods. To our best knowledge,  
2 this is the first report of cell volume oscillation in *D. salina* when growing under diurnal conditions.  
3 Since *D. salina* cells lack a rigid polysaccharide cell wall, their cytoplasmic membranes allow the  
4 cells to adjust their volume and shape rapidly in response to the environmental changes (Maeda and  
5 Thompson, 1986). Although early studies have reported rhythmic changes in cell shapes of *Euglena*  
6 *gracilis* (Lonergan, 1983), the mechanism in *E. gracilis* is different to that in *D. salina* reported in  
7 this study. *E. gracilis* cell shape is under direct control of the biological clock and thus even under  
8 continuous light, the daily rhythm of cell shape remains. However, when *D. salina* was grown  
9 under continuous light, the oscillation in cell shape ceased (Fig. 1), indicating that it is under the  
10 control of diurnal change rather than circadian rhythm, or due to cell division. The oscillation in cell  
11 volume and cellular glycerol content of CCAP 19/30 is not found in several other *Dunaliella*  
12 species maintained in the laboratory, including *D. parva*, *D. quartolecta*, and *D. polymorpha* nor in  
13 green microalga *Chlamydomonas reinhardtii* (data not shown); and since no previous report has  
14 been found, it may be a species specific property.

15         The synthesis or degradation of glycerol in response to osmotic pressure change is  
16 commonly assumed to be triggered by cell volume change (Ben-Amotz and Avron, 1981; Zelazny  
17 et al., 1995). However in this study, we show by using light/dark cycles that the change in cell  
18 volume can also be the result of change in cellular glycerol content. Glycerol is produced by  
19 *Dunaliella* via photosynthesis and the adjustment in glycerol concentration is achieved by  
20 regulating the carbon flux between either the synthesis of starch or glycerol (Goyal, 2007b; 2007a).  
21 In the dark, there is no carbon fixed to glycerol from photosynthesis, and starch is respired to  
22 produce energy and metabolites: the pool size of glycerol is thus reduced. This causes the cell  
23 volume to decrease in the dark to maintain the osmotic pressure. With further time in the dark an  
24 apparent increase in cellular glycerol and starch contents was observed: this seemingly counter-  
25 intuitive observation may nevertheless be due to additional dark-related events such as the effects of  
26 lipid catabolism in photoautotrophic algae that have been deprived of an external carbon and energy  
27 source, releasing fatty acids and glycerol.

1 It is well documented that exposure of chloroplasts to high light leads to PSII photodamage  
2 when the rate of photodamage exceeds that of the repair cycle, leading to photoinhibition and  
3 reduced photosynthetic efficiency (Melis, 1999; Yokthongwattana and Melis, 2008). For the higher  
4 plant *Arabidopsis thaliana*, the rate of photodamage dominates in light intensities greater than 500  
5  $\mu\text{mol photons} \cdot \text{m}^{-2} \cdot \text{s}^{-1}$  and leads to photoinhibition (Havaux et al., 2000). In our study, light  
6 intensity at all values above 500  $\mu\text{mol photons} \cdot \text{m}^{-2} \cdot \text{s}^{-1}$  resulted in a decrease in the ratio of Fv/Fm  
7 by about 34 % compared to that at 200  $\mu\text{mol photons} \cdot \text{m}^{-2} \cdot \text{s}^{-1}$  indicating PSII damage. The  
8 decreased photosynthetic rate observed for cultures acclimated to light intensities of 200 and 500  
9  $\mu\text{mol photons} \cdot \text{m}^{-2} \cdot \text{s}^{-1}$  is therefore likely to be due to photoinhibition. At higher light intensities,  
10 however, photosynthetic rate increased to a maximum level (Fig. 6A and 6B). This finding implies  
11 that CCAP 19/30 might have evolved an efficient repair cycle that allows it to turnover damaged  
12 PSII at a much faster rate at high light intensity to allow it to maintain maximum photosynthetic  
13 efficiency. Indeed, it has been shown that *Dunaliella tertiolecta* was able to recover the PS II  
14 efficiency by 80 % from photodamage within just 1 minute of dark adaption (Casper-Lindley and  
15 Björkman, 1998).

16 The enhanced rate of photosynthesis at high light intensities in this study contributed to the  
17 tolerance of CCAP 19/30 to photodamage. The rate of photodamage is dependent upon  $Q_A$  redox  
18 state, occurring at low probability when  $Q_A$  is oxidized and excitation energy is utilized in the  
19 electron transport chain at a much faster rate (Melis, 1999). Increase in the photosynthetic rate  
20 therefore leads to rapid oxidation of the PQ-pool, which in turn drains electrons at a much faster  
21 rate from the  $Q_A$  site of PSII, reducing the possibility of PSII-photodamage. The ability of *D. salina*  
22 to enhance photosynthetic activity under stressed conditions has been previously reported by Liska  
23 et al. (Liska et al., 2004). In their study, the enhanced photosynthesis was found to contribute to  
24 salinity tolerance of *D. salina* and cells grown at high salinity showed enhancement of  $\text{CO}_2$   
25 assimilation, starch mobilization as well as up regulated key enzymes in photosynthesis.

26 When exposed to high light, the *Dunaliella* cells are reported to use the carotenoid synthesis  
27 pathway as a protective mechanism against photodamage (Kim et al., 2013; Mulders et al., 2014;

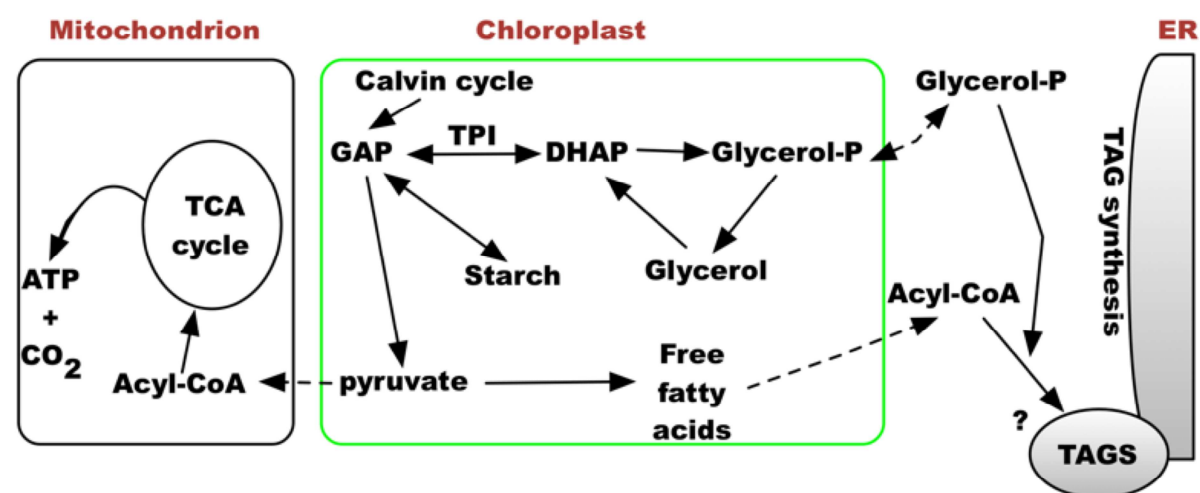
1 Park et al., 2013; Salguero et al., 2003). Different *Dunaliella* strains may vary significantly in their  
2 response to light stress and show different sensitivity to the light intensities. In this study, the strain  
3 CCAP 19/30 only shows a slight increase in the carotenoids/chlorophyll ratio with both carotenoids  
4 and chlorophyll content decreased due to photoinhibition (Table 1). This suggests that carotenoid  
5 synthesis in this strain may not be the main functioning mechanism to protect cells from high light  
6 stress. Instead, the >2-fold increase in cellular glycerol content at high light indicates glycerol may  
7 act as a chemical chaperone to maintain photosynthetic efficiency at high light. In a previous study  
8 by Yilancioglu et al. (Yilancioglu et al., 2014), a strong correlation between glycerol production and  
9 the maximum and effective photosynthetic yield parameters showed that glycerol plays an  
10 important role not only in regulating the osmotic balance but also determining the yield and  
11 biochemical composition of the biomass under oxidative stress.

12 Glycerol synthesis in *Dunaliella* species as a response to osmotic stress has been intensively  
13 studied. Upon hyperosmotic stress, *Dunaliella* cells respond immediately by reducing their cell  
14 volume due to water efflux across the cell membrane (Chen and Jiang, 2009). Plasma membrane  
15 sterols sense the cell volume change and trigger the synthesis of glycerol (Zelazny et al., 1995). In  
16 the present study, increasing cellular concentration of glycerol correlated positively with  
17 photodamage to the cells cultured under different light intensities, as indicated by the Fv/Fm values  
18 (Fig. 5). At the same time results in this study show that with high light stress, photosynthesis is  
19 enhanced and that the increase in photosynthesis was accompanied by an increase in dark  
20 respiration rate (Fig. 6C and 6D) and glycerol synthesis (Fig. 7A and 7B). The faster growth rate in  
21 high light (Fig. 4) shows energy demand is higher, and was probably met by the faster carbon  
22 assimilation and respiration (Fig. 6). These findings accord with a previous study which found that  
23 *Dunaliella* cells contained higher glycerol contents at higher light intensities (Davis et al., 2015).  
24 The higher cellular glycerol content of cells grown at high light intensities also indicates larger cell  
25 diameters at high light, as shown in Table 1, the average cell volume of cells indeed increases with  
26 the light intensity, which is in line with the study on *D. salina* CCAP 19/18 by Park et al. (Park et  
27 al., 2013). However, despite the significant increase in cellular glycerol content at 1000 and 1500

1  $\mu\text{mol photons} \cdot \text{m}^{-2} \cdot \text{s}^{-1}$  (about 2-fold of that at 50, 200 and 500  $\mu\text{mol photons} \cdot \text{m}^{-2} \cdot \text{s}^{-1}$ ), the cell

2 volume did not show such a significant increase with light (Table 1), indicating that glycerol  
3 functions as more than an osmolyte to balance the osmotic pressure in CCAP 19/30, but also a  
4 protecting mechanism when under high light stress.

5



6

7 **Fig. 8.** A schematic diagram showing the working model of CCAP 19/30 carrying out higher  
8 photosynthetic efficiency at high light intensity via increased glycerol synthesis and respiration.

9

10 In Fig. 8 we propose a working model in which CCAP 19/30 uses glycerol in metabolic  
11 homeostasis because glycerol synthesis is able to reduce the possibility of photoinhibition by  
12 draining electrons from the Q<sub>A</sub> site from photosynthesis (Fig. 7). Thus in light, dihydroxyacetone  
13 phosphate (DHAP), the precursor of glycerol is isomerised rapidly and reversibly by triose  
14 phosphate isomerase from glyceraldehyde-3-phosphate (GAP), the export product of the Calvin  
15 cycle in photosynthesis placing an energy demand on the cell, whilst glycerol synthesis from DHAP  
16 requires reducing equivalents (NADH or FADH<sub>2</sub>) for glycerol phosphate dehydrogenase  
17 functionality. The parallel increase in respiration (Fig. 6C and 6D) suggests that synthesized  
18 glycerol might be used for anabolic metabolism via oxidative respiration using the mitochondrial  
19 citric acid cycle. The actual pool size of glycerol however could be a reflection of multiple survival

1 strategies under high light intensity since glycerol can also be used for membrane (triglyceride)  
2 regeneration, or stored in the form of starch. In some lipid-storing green algae (Combe et al., 2015;  
3 Yilancioglu et al., 2014) oxidative stress either caused by nitrogen depletion or by exposure to  
4 excess light or by application of exogenous H<sub>2</sub>O<sub>2</sub> is correlated with an increase in triglycerides  
5 content (but also see (Ben-Amotz et al., 1985)). Glycerol can also serve as a biocompatible solute or  
6 chemical chaperone to assist in refolding damaged proteins (Lamitina et al., 2006). Clearly glycerol  
7 has multiple functions that serve to protect and maintain growth of CCAP 19/30 cells not only in  
8 conditions of high salinity but also under high light intensities.

9

#### 10 **Acknowledgement**

11 This research was supported by a grant to Prof. Patricia Harvey as part of Ecotec21 a project  
12 selected under the European Cross-border Cooperation Programme INTERREG IV A France  
13 (Channel) – England, co-funded by the European Régional Development Fund and by grant  
14 agreement no. 613870 awarded under FP7 KBBE.2013.3.2-02. The authors would like to express  
15 their sincere gratitude to Prof. Ami Ben-Amotz, Dr John Milledge and to Dr Elinor P Thompson for  
16 invaluable discussion and to Dr Paul Dyer for his assistance with the flow cytometer analysis  
17 undertaken.

18

#### 19 **References**

- 20 Alkayal, F., Albion, R.L., Tillett, R.L., Hathwaik, L.T., Lemos, M.S., Cushman, J.C., 2010.  
21 Expressed sequence tag (EST) profiling in hyper saline shocked *Dunaliella salina* reveals high  
22 expression of protein synthetic apparatus components. *Plant Sci.* 179, 437–449.  
23 doi:10.1016/j.plantsci.2010.07.001
- 24 Barker, J.P., Cattolico, R.A., Gatza, E., 2012. Multiparametric analysis of microalgae for biofuels  
25 using flow cytometry.
- 26 Baroli, I., Melis, A., 1998. Photoinhibitory damage is modulated by the rate of photosynthesis and  
27 by the photosystem II light-harvesting chlorophyll antenna size. *Planta* 205, 288–296.

- 1 Ben-Amotz, A., Avron, M., 1981. Glycerol and  $\beta$ -carotene metabolism in the halotolerant alga  
2 *Dunaliella*: a model system for biosolar energy conversion. Trends Biochem. Sci. 6, 297–299.  
3 doi:10.1016/0968-0004(81)90106-7
- 4 Ben-Amotz, A., Katz, A., Avron, M., 1982a. Accumulation of  $\beta$ -carotene in halotolerant alga:  
5 purification and characterization of  $\beta$ -carotene-rich globules from *Dunaliella bardawil*  
6 (chlorophyceae). J. Phycol. 18, 529–537. doi:10.1111/j.1529-8817.1982.tb03219.x
- 7 Ben-Amotz, A., Sussman, I., Avron, M., 1982b. Glycerol production by *Dunaliella*. Experientia 38,  
8 49–52. doi:10.1007/BF01944527
- 9 Ben-Amotz, A., Tornabene, T.G., Thomas, W.H., 1985. Chemical profile of selected species of  
10 microalgae with emphasis on lipids. J. Phycol. 21, 72–81. doi:10.1111/j.0022-  
11 3646.1985.00072.x
- 12 Bondioli, P., Bella, Della, L., 2005. An alternative spectrophotometric method for the determination  
13 of free glycerol in biodiesel. Eur. J. Lipid Sci. Technol. 107, 153–157.  
14 doi:10.1002/ejlt.200401054
- 15 Borowitzka, M.A., 1988. Algal growth media and sources of cultures, in: Borowitzka, M.A.,  
16 Borowitzka, L.J. (Eds.), Microalgal Biotechnology. pp. 456–465.
- 17 Brindley, C., Ación, F.G., Fernández Sevilla, J.M., 2010. The oxygen evolution methodology  
18 affects photosynthetic rate measurements of microalgae in well-defined light regimes.  
19 Biotechnol. Bioeng. 106, 228–237. doi:10.1002/bit.22676
- 20 Casper-Lindley, C., Björkman, O., 1998. Fluorescence quenching in four unicellular algae with  
21 different light-harvesting and xanthophyll-cycle pigments. Photosyn. Res. 56, 277–289.
- 22 Chen, H., Jiang, J.-G., 2009. Osmotic responses of *Dunaliella* to the changes of salinity. J. Cell.  
23 Physiol. 219, 251–258. doi:10.1002/jcp.21715
- 24 Chitlaru, E., Pick, U., 1991. Regulation of glycerol synthesis in response to osmotic changes in  
25 *Dunaliella*. Plant Physiol. 96, 50–60.
- 26 Combe, C., Hartmann, P., Rabouille, S., Talec, A., Bernard, O., Sciandra, A., 2015. Long-term  
27 adaptive response to high-frequency light signals in the unicellular photosynthetic eukaryote

- 1 *Dunaliella salina*. Biotechnol. Bioeng. 112, 1111–1121. doi:10.1002/bit.25526
- 2 Davidi, L., Levin, Y., Ben-Dor, S., Pick, U., 2014. Proteome analysis of cytoplasmatic and plastidic  
3  $\beta$ -carotene lipid droplets in *Dunaliella bardawil*. Plant Physiol. 167, 60–79.  
4 doi:10.1104/pp.114.248450
- 5 Davis, R.W., Carvalho, B.J., Jones, H.D.T., Singh, S., 2015. The role of photo-osmotic adaptation  
6 in semi-continuous culture and lipid particle release from *Dunaliella viridis*. J. Appl. Phycol. 27,  
7 109–123. doi:10.1007/s10811-014-0331-5
- 8 Delieu, T.J., Walker, D.A., 1983. Simultaneous measurement of oxygen evolution and chlorophyll  
9 fluorescence from leaf. Plant Physiol. 73, 534–541.
- 10 Dixon, L.E., Hodge, S.K., van Ooijen, G., Troein, C., Akman, O.E., Millar, A.J., 2014. Light and  
11 circadian regulation of clock components aids flexible responses to environmental signals. New  
12 Phytol. 203, 568–577. doi:10.1111/nph.12853
- 13 Duanmu, D., Bachy, C., Sudek, S., Wong, C.-H., Jiménez, V., Rockwell, N.C., Martin, S.S., Ngan,  
14 C.Y., Reistetter, E.N., van Baren, M.J., Price, D.C., Wei, C.-L., Reyes-Prieto, A., Lagarias, J.C.,  
15 Worden, A.Z., 2014. Marine algae and land plants share conserved phytochrome signaling  
16 systems. Proc. Natl. Acad. Sci. U.S.A. 201416751. doi:10.1073/pnas.1416751111
- 17 Genty, B., Briantais, J.-M., Baker, N.R., 1989. The relationship between the quantum yield of  
18 photosynthetic electron transport and quenching of chlorophyll fluorescence. Biochim. Biophys.  
19 Acta, Gen. Subj. 990, 87–92. doi:10.1016/S0304-4165(89)80016-9
- 20 Goyal, A., 2007a. Osmoregulation in *Dunaliella*, part I: effects of osmotic stress on photosynthesis,  
21 dark respiration and glycerol metabolism in *Dunaliella tertiolecta* and its salt-sensitive mutant  
22 (HL 25/8). Plant Physiol. Biochem. 45, 696–704. doi:10.1016/j.plaphy.2007.05.008
- 23 Goyal, A., 2007b. Osmoregulation in *Dunaliella*, part II: photosynthesis and starch contribute  
24 carbon for glycerol synthesis during a salt stress in *Dunaliella tertiolecta*. Plant Physiol.  
25 Biochem. 45, 705–710. doi:10.1016/j.plaphy.2007.05.009
- 26 Havaux, M., Bonfils, J.P., Lütz, C., Niyogi, K.K., 2000. Photodamage of the photosynthetic  
27 apparatus and its dependence on the leaf developmental stage in the npq1 *Arabidopsis* mutant

- 1 deficient in the xanthophyll cycle enzyme violaxanthin de-epoxidase. *Plant Physiol.* 124, 273–  
2 284.
- 3 Kim, S.-H., Liu, K.-H., Lee, S.-Y., Hong, S.-J., Cho, B.-K., Lee, H., Lee, C.-G., Choi, H.-K., 2013.  
4 Effects of light intensity and nitrogen starvation on glycerolipid, glycerophospholipid, and  
5 carotenoid composition in *Dunaliella tertiolecta* culture. *PLoS ONE* 8, e72415.  
6 doi:10.1371/journal.pone.0072415
- 7 Lamitina, T., Huang, C.G., Strange, K., 2006. Genome-wide RNAi screening identifies protein  
8 damage as a regulator of osmoprotective gene expression. *PNAS* 103, 12173–12178.  
9 doi:10.1073/pnas.0602987103
- 10 Lin, H., Fang, L., Low, C.S., Chow, Y., Lee, Y.K., 2013. Occurrence of glycerol uptake in  
11 *Dunaliella tertiolecta* under hyperosmotic stress. *FEBS J.* 280, 1064–1072.  
12 doi:10.1111/febs.12100
- 13 Liska, A.J., Shevchenko, A., Pick, U., Katz, A., 2004. Enhanced photosynthesis and redox energy  
14 production contribute to salinity tolerance in *Dunaliella* as revealed by homology-based  
15 proteomics. *Plant Physiol.* 136, 2806–2817. doi:10.1104/pp.104.039438
- 16 Lonergan, T.A., 1983. Regulation of cell shape in *Euglena gracilis*: I. involvement of the biological  
17 clock, respiration, photosynthesis, and cytoskeleton. *Plant Physiol.* 71, 719–730.  
18 doi:10.1104/pp.71.4.719
- 19 Maeda, M., Thompson, G.A., 1986. On the mechanism of rapid plasma membrane and chloroplast  
20 envelope expansion in *Dunaliella salina* exposed to hypoosmotic shock. *J. Cell Biol.* 102, 289–  
21 297.
- 22 Matsuo, T., Ishiura, M., 2011. *Chlamydomonas reinhardtii* as a new model system for studying the  
23 molecular basis of the circadian clock. *FEBS Lett.* 585, 1495–1502.  
24 doi:10.1016/j.febslet.2011.02.025
- 25 Melis, A., 1999. Photosystem-II damage and repair cycle in chloroplasts: what modulates the rate of  
26 photodamage ? *Trends Plant Sci.* 4, 130–135.
- 27 Mimuro, M., Akimoto, S., 2003. Carotenoids of light harvesting systems: energy transfer processes

- 1 from fucoxanthin and peridinin to chlorophyll, in: *Photosynthesis in Algae*. Springer  
2 Netherlands, Dordrecht, pp. 335–349. doi:10.1007/978-94-007-1038-2\_15
- 3 Mulders, K.J.M., Lamers, P.P., Martens, D.E., Wijffels, R.H., 2014. Phototrophic pigment  
4 production with microalgae: biological constraints and opportunities. *J. Phycol.* 50, 229–242.  
5 doi:10.1111/jpy.12173
- 6 Park, S., Lee, Y., Jin, E., 2013. Comparison of the responses of two *Dunaliella* strains, *Dunaliella*  
7 *salina* CCAP 19/18 and *Dunaliella bardawil* to light intensity with special emphasis on  
8 carotenogenesis. *ALGAE* 28, 203–211.
- 9 Porra, R.J., Thompson, W.A., Kriedemann, P.E., 1989. Determination of accurate extinction  
10 coefficients and simultaneous equations for assaying chlorophylls a and b extracted with four  
11 different solvents: verification of the concentration of chlorophyll standards by atomic  
12 absorption spectroscopy. *Biochim. Biophys. Acta, Bioenerg.* 975, 384–394. doi:10.1016/S0005-  
13 2728(89)80347-0
- 14 Priyadarshani, I., Rath, B., 2012. Bioactive compounds from microalgae and cyanobacteria: utility  
15 and applications. *Int. J. Pharm. Sci. Res.* 3, 4123–4130.
- 16 Raja, R., Hemaiswarya, S., Kumar, N.A., Sridhar, S., Rengasamy, R., 2008. A perspective on the  
17 biotechnological potential of microalgae. *Crit. Rev. Microbiol.* 34, 77–88.  
18 doi:10.1080/10408410802086783
- 19 Sadka, A., Lers, A., Zamir, A., Avron, M., 1989. A critical examination of the role of de novo  
20 protein synthesis in the osmotic adaptation of the halotolerant alga. *FEBS Lett.* 244, 93–98.
- 21 Salguero, A., la Morena, de, B., Vigar, J., Vega, J.M., Vílchez, C., León, R., 2003. Carotenoids as  
22 protective response against oxidative damage in *Dunaliella bardawil*. *Biomol. Eng.* 20, 249–  
23 253. doi:10.1016/S1389-0344(03)00065-0
- 24 Sorokina, O., Corellou, F., Dauvillée, D., Sorokin, A., Goryanin, I., Ball, S., Bouget, F.-Y., Millar,  
25 A.J., 2011. Microarray data can predict diurnal changes of starch content in the picoalga  
26 *Ostreococcus*. *BMC Syst. Biol.* 5, 36. doi:10.1186/1752-0509-5-36
- 27 Spolaore, P., Joannis-Cassan, C., Duran, E., Isambert, A., 2006. Commercial applications of

- 1 microalgae. J. Biosci. Bioeng. 101, 87–96. doi:10.1263/jbb.101.87
- 2 Strickland, J., Parsons, T.R., 1972. A practical handbook of seawater analysis, 2nd ed. Fish Res  
3 Board Can Bull.
- 4 Sun, J., Liu, D., 2003. Geometric models for calculating cell biovolume and surface area for  
5 phytoplankton. J. Plankton Res. 25, 1331–1346. doi:10.1093/plankt/fbg096
- 6 Tafreshi, A.H., Shariati, M., 2009. *Dunaliella* biotechnology: methods and applications. J. Appl.  
7 Microbiol. 107, 14–35. doi:10.1111/j.1365-2672.2009.04153.x
- 8 Wahidin, S., Idris, A., Shaleh, S.R.M., 2013. The influence of light intensity and photoperiod on the  
9 growth and lipid content of microalgae *Nannochloropsis* sp. Bioresour. Technol. 129, 7–11.  
10 doi:10.1016/j.biortech.2012.11.032
- 11 Xu, Y., Milledge, J.J., Abubakar, A., Swamy, R.A.R., Bailey, D., Harvey, P.J., 2015. Effects of  
12 centrifugal stress on cell disruption and glycerol leakage from *Dunaliella salina*. Microalgae  
13 Biotechnology 1, 20–27. doi:10.1515/micbi-2015-0003
- 14 Yilancioglu, K., Cokol, M., Pastirmaci, I., Erman, B., Cetiner, S., 2014. Oxidative stress is a  
15 mediator for increased lipid accumulation in a newly isolated *Dunaliella salina* strain. PLoS  
16 ONE 9, e91957. doi:10.1371/journal.pone.0091957
- 17 Yokthongwattana, K., Melis, A., 2008. Photoinhibition and recovery in oxygenic photosynthesis:  
18 mechanism of a photosystem II damage and repair cycle, in: Photoprotection, Photoinhibition,  
19 Gene Regulation, and Environment, Advances in Photosynthesis and Respiration. Springer  
20 Netherlands, Dordrecht, pp. 175–191. doi:10.1007/1-4020-3579-9\_12
- 21 Zelazny, A.M., Shaish, A., Pick, U., 1995. Plasma membrane sterols are essential for sensing  
22 osmotic changes in the halotolerant alga *Dunaliella*. Plant Physiol. 109, 1395–1403.
- 23 Zhao, L., Gong, W., Chen, X., Chen, D., 2013. Characterization of genes and enzymes in  
24 *Dunaliella salina* involved in glycerol metabolism in response to salt changes. Phycol. Res. 61,  
25 37–45. doi:10.1111/j.1440-1835.2012.00669.x
- 26

**Highlights**

- Cell volume oscillates with the light/dark cycle in *D. salina* CCAP 19/30
- Cell volume and glycerol oscillations are under diurnal control
- Glycerol increased >2-fold when light intensity doubled to 1000  $\mu\text{mol photons m}^{-2}\text{s}^{-1}$
- Glycerol stabilized the photosynthetic apparatus in high intensity light

**Contribution**

Yanan Xu and Iskander M. Ibrahim were responsible for design of and conducting the experiments and preparation of the manuscript

Patricia J. Harvey was responsible for planning, analysis of data and preparation of the manuscript

ACCEPTED MANUSCRIPT